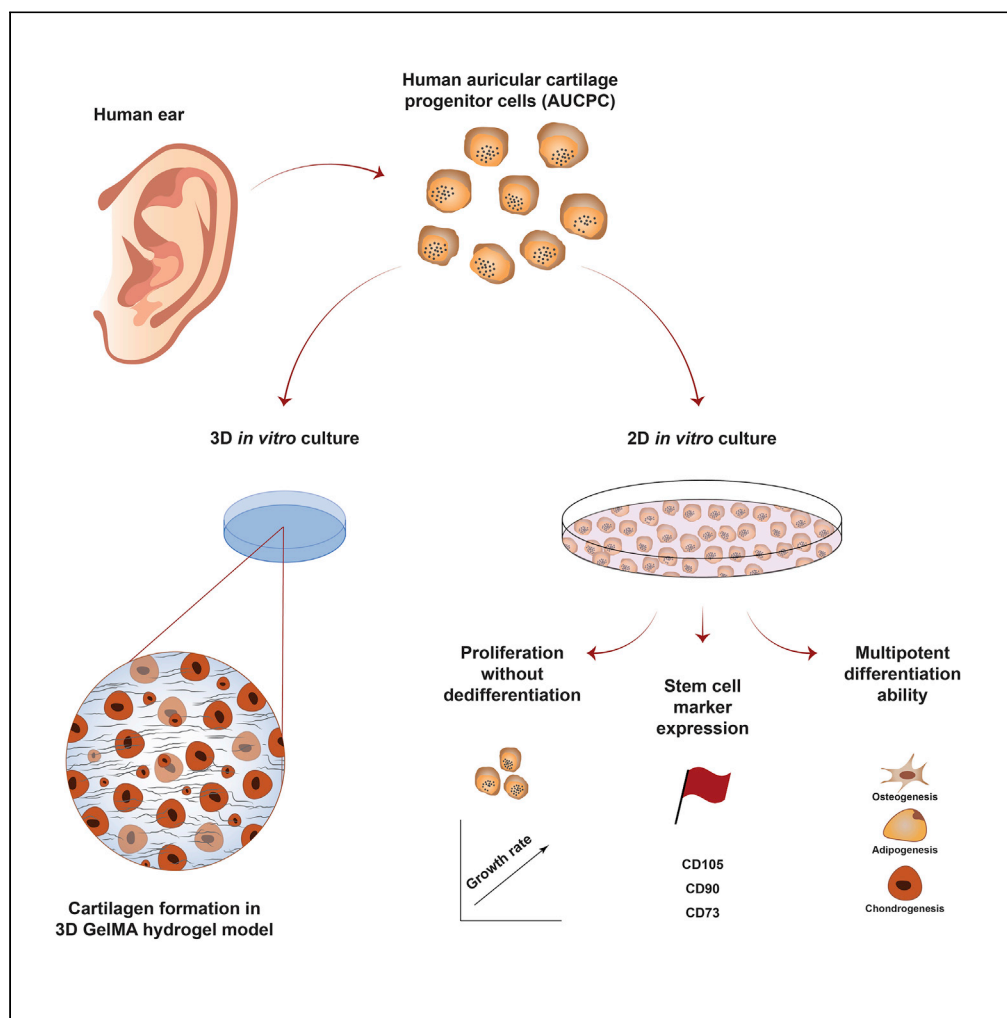**Article**

Human adult, pediatric and microtia auricular cartilage harbor fibronectin-adhering progenitor cells with regenerative ear reconstruction potential

Human ear

Human auricular cartilage progenitor cells (AUCPC)

3D *in vitro* culture

2D *in vitro* culture

Cartilagen formation in 3D GelMA hydrogel model

Proliferation without dedifferentiation

Growth rate

Stem cell marker expression

CD105
CD90
CD73

Multipotent differentiation ability

Osteogenesis
Adipogenesis
Chondrogenesis

Iris A. Otto,
Paulina Nuñez
Bernal, Margot
Rikkers, ...,
Corstiaan C.
Breugem,
Riccardo Levato,
Jos Malda

r.levato@uu.nl (R.L.)
j.malda@umcutrecht.nl (J.M.)

Highlights

First identification of cartilage progenitor cells in human auricular cartilage

Microtia cartilage remnant also contains regenerative progenitor cells

AuCPCs exhibit potent proliferation ability without dedifferentiation

AuCPCs produce elastic-type cartilage-like matrix in 3D culture

Article

Human adult, pediatric and microtia auricular cartilage harbor fibronectin-adhering progenitor cells with regenerative ear reconstruction potential

Iris A. Otto,[1,2] Paulina Nuñez Bernal,[1] Margot Rikkers,[1] Mattie H.P. van Rijen,[1] Anneloes Mensinga,[1] Moshe Kon,[2] Corstiaan C. Breugem,[3] Riccardo Levato,[1,4,5,*] and Jos Malda[1,4,*]

SUMMARY

Remaining challenges in auricular cartilage tissue engineering include acquiring sufficient amounts of regeneration-competent cells and subsequent production of high-quality neocartilage. Progenitor cells are a resident subpopulation of native cartilage, displaying a high proliferative and cartilage-forming capacity, yet their potential for regenerative medicine is vastly understudied. In this study, human auricular cartilage progenitor cells were newly identified in healthy cartilage and, importantly, in microtia-impaired chondral remnants. Their cartilage repair potential was assessed via *in vitro* 3D culture upon encapsulation in a gelatin-based hydrogel, and subsequent biochemical, mechanical, and histological analyses. Auricular cartilage progenitor cells demonstrate a potent ability to proliferate without losing their multipotent differentiation ability and to produce cartilage-like matrix in 3D culture. As these cells can be easily obtained through a non-deforming biopsy of the healthy ear or from the otherwise redundant microtia remnant, they can provide an important solution for long-existing challenges in auricular cartilage tissue engineering.

INTRODUCTION

Microtia is a developmental disorder of the external ear, which results in a range of auricular deformities spanning from minimal structural anomalies to a complete absence of the auricle. Worldwide, 0.8–4.2 per 10.000 children are born with this usually unilateral condition (Alasti and Van Camp, 2009). Although relatively uncommon, having this visible deformity is burdensome for both children and adults. The unusual appearance of the auricle often causes teasing and a reduced self-confidence, impacting social life, career, and leisure activities. Anxiety, depression, and behavioral problems are also reported in patients with microtia (Horlock et al., 2005). Psychosocial functioning improves significantly after surgical correction of the affected ear (Horlock et al., 2005; Steffen et al., 2010; Johns et al., 2015).

The current golden standard in the treatment of microtia is auricular reconstruction surgery using autologous cartilage tissue. In this procedure, cartilage grafts are taken from the patient's ribs and skillfully carved into a framework that mimics the contours of the contralateral normal ear (Bauer, 2009). Although decent aesthetic results can be obtained with this approach, there are important drawbacks. Firstly, as the ear is as unique as a fingerprint (Hurley et al., 2008), auricular reconstruction is perceived as one of the most challenging procedures in plastic surgery (Magritz and Siegert, 2014). Even in experienced hands, the results from reconstructive surgery are not always consistent (Bauer, 2009). Secondly, the carved framework is considerably different from the delicate three-dimensional structure of the native auricle in terms of fine anatomy and mechanical properties: the reconstructed fibrocartilage framework is slightly thicker and less flexible in comparison to the native elastic cartilage. In addition, symmetrical projection from the skull is difficult to achieve (Bichara et al., 2012; Jessop et al., 2016). As the costal cartilage is prone to calcification, over time the definition of the carved frame can become less pronounced and more rigid (Jessop et al., 2016). Thirdly, there is a risk of post-operative infection at both operative sites or necrosis of the skin overlying the cartilage frame. Lastly, harvesting a large chunk of cartilage from the ribs can cause a visible chest deformity, a wide scar on the chest, and has a risk of complications including pneumothorax (Jessop et al., 2016; Ciorba and Martini, 2006). Synthetic implants such as those made of silicone or porous polyethylene eliminate donor site morbidity and framework problems from the equation, yet they are still deemed less

[1]Department of Orthopaedics, University Medical Center Utrecht, Heidelberglaan 100, Utrecht, 3584 CX, the Netherlands

[2]Department of Plastic, Reconstructive and Hand Surgery, University Medical Center Utrecht, Heidelberglaan 100, Utrecht, 3584 CX, the Netherlands

[3]Department of Plastic, Reconstructive and Hand Surgery, Amsterdam University Medical Center, Emma Children's Hospital, Meibergdreef 9, Amsterdam, 1105 ZA, the Netherlands

[4]Department of Clinical Sciences, Faculty of Veterinary Science, Utrecht University, Yalelaan 108, Utrecht, 3584 CM, the Netherlands

[5]Lead contact

*Correspondence:
r.levato@uu.nl (R.L.),
j.malda@umcutrecht.nl (J.M.)

https://doi.org/10.1016/j.isci.2022.104979

favorable due to risk of implant fracture and occurrences of extrusion through the skin after infection or light traumas (Bauer, 2009; Cenzi et al., 2005; Baluch et al., 2014).

Tissue-engineered implants can open new avenues to overcome the aforementioned donor site morbidity and unsatisfactory aesthetic outcomes related to the current treatment. Tissue engineering technologies allow for the creation of new cartilage *in vitro* by using a combination of cells, bioactive cues, and supporting materials to grow new tissue (Langer and Vacanti, 1993; Kuo et al., 2006). Using these principles as a therapeutic approach would obviate harvesting and sculpting the costal cartilage framework, consequently decreasing operating time and avoiding donor site morbidity. Despite great advances in cartilage tissue engineering, two main challenges in engineering the elastic cartilage of the human auricle remain. Firstly, a significant number of cells are required for the generation of a cartilage construct the size of the human auricle: estimates range between 100 and 250 million cells (Bichara et al., 2012; Cohen et al., 2018). Secondly, the quality of engineered cartilage is still suboptimal with regards to structure, component ratios, biocompatibility, functionality, and durability (Bichara et al., 2012; Otto et al., 2015; Nayyer et al., 2012; Sterodimas et al., 2009). Specifically, the neotissue often exhibits fibrous characteristics or calcifications (Jessop et al., 2016; Saim et al., 2000; Kamil et al., 2003; Kusuhara et al., 2008; Bichara et al., 2014). In addition, a critical characteristic of the external ear is its flexibility, allowing the auricle to bend without breaking. This flexibility is achieved through the presence of elastic fibers in the tissue, which is accordingly classified as elastic cartilage (Bichara et al., 2012; Griffin et al., 2016; Zopf et al., 2015; Nimeskern et al., 2014; Pappa et al., 2013; Roy et al., 2004). Hence, the production of elastic fibers in engineered cartilage tissue will greatly contribute to the construct's flexibility. The overall success of a tissue-engineered auricular cartilage implant is largely determined by the quality of the produced tissue. Consequently, choosing an appropriate cell type is crucial in overcoming the hurdles of quantity and quality.

Cell-based tissue engineering of the human auricle thus requires a high cell yield and the ability of the chosen cell type to produce cartilage-specific extracellular matrix to recapitulate the biochemical and mechanical properties of the native elastic auricular cartilage. Options include primary chondrocytes, mesenchymal stromal cells (MSC), and more recently also cartilage progenitor cells (CPC). Chondrocytes naturally possess a chondrogenic determination, yet they rapidly lose their phenotype upon expansion *in vitro* (Phull et al., 2016; Schnabel et al., 2002; Homicz et al., 2002; Saadeh et al., 1999). As such, the use of this cell type would require a very large donor site in order to obtain a sufficient number of cells to create the human auricle. Mesenchymal stem cells, in contrast, have a high expansion capacity *in vitro* (Gardner et al., 2013) but exhibit a tendency to undergo hypertrophic differentiation upon long-term *in vitro* and *in vivo* culture, which can result in the formation of calcified cartilage. This template can then be remodeled into bone through the process of endochondral ossification, leading to undesirable tissue calcifications contributing to implant stiffness (Gawlitta et al., 2010; Mueller and Tuan, 2008). Despite numerous strategies, including redifferentiation of chondrocytes (Mandl et al., 2002; Pomerantseva et al., 2016; Tay et al., 2004; Tseng et al., 2014; van Osch et al., 2001) or co-culturing MSCs with chondrocytes (Cohen et al., 2018; Kang et al., 2012; Liu et al., 2010; Pleumeekers et al., 2015; Zhang et al., 2014), translation of tissue-engineered auricular cartilage toward clinical application remains hampered by the requisite of sufficient cell quantities able to produce adequate quality neocartilage.

Cartilage progenitor cells originate in the native cartilage tissue and have been shown to exhibit a high proliferative capacity and to retain multipotency upon expansion (Williams et al., 2010; Xue et al., 2016; Rikkers et al., 2021). In our previous studies, CPCs isolated from equine auricular and articular cartilage have been shown to produce cartilage-like tissue in an *in vitro* 3D hydrogel model (Otto et al., 2018; Levato et al., 2017). In addition, equine auricular CPCs were shown to exhibit a significant reduction of the expression of RUNX2—the master transcription factor for hypertrophy and osteogenesis—compared to its expression by MSCs (Otto et al., 2018). Similar results were found in a study comparing articular cartilage progenitor cells and MSCs (Vinod et al., 2021). In addition, a study using fibronectin-adhering nasoseptal chondroprogenitors indicated the importance of these cells for phenotypic stability of the newly formed cartilage tissue (Jessop et al., 2020). The results of these studies supply encouraging results for the use of cartilage progenitor cells as an alternative cell source to chondrocytes and MSCs for auricular cartilage tissue engineering.

The purpose of the current study was to identify CPCs in the human auricular cartilage and to assess their potential for cartilage regeneration. We describe the presence of auricular cartilage progenitor cells (AuCPC) in human auricular cartilage from different donor sources. The proliferative and multipotent
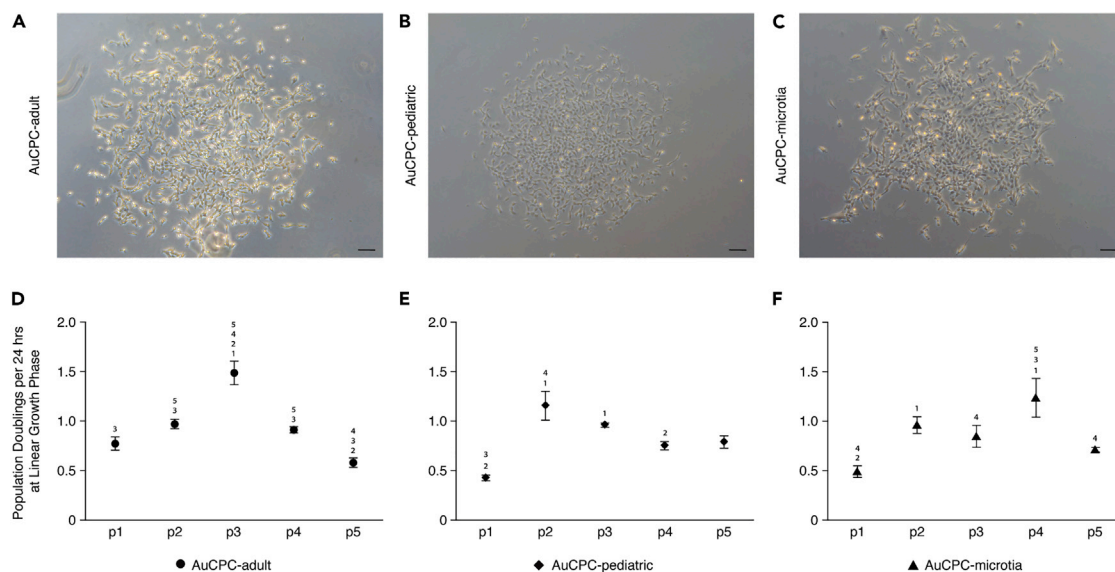
Figure 1. Colony formation capacity and proliferation rates
Isolated progenitor cells sourced from (A) adult, (B) pediatric, and (C) microtia cartilage demonstrated the ability to form colonies at passage 0. Scale bars represent 100 μm. Proliferation rates were determined at passages 1–5 and are presented as population doublings per 24 h for (D) adult, (E) pediatric, and (F) microtia progenitors. Data are represented as mean +/- SEM. Analyses were performed through two-way ANOVA with a Bonferroni post-hoc test. Statistically significant differences of $p < 0.05$ are indicated by numbers that refer to the compared passage number (*e.g.* 1 represents a significant difference to p1). Letters refer to donor group (A = adult, P = pediatric, M = microtia) and indicate significant differences within the passage.

qualities of progenitors sourced from adult, pediatric, and rudimentary microtia auricular cartilage were characterized throughout multiple passages. In addition, cells were encapsulated in a 3D hydrogel system and cultured in chondrogenic differentiation medium for a period of 56 days during which biochemical, mechanical, and histological assessment was performed to evaluate the chondrogenic capacity of these cells for use in tissue engineering strategies.

RESULTS

Human auricular cartilage progenitor cells demonstrate stem cell potency

Progenitor cells isolated from the auricular cartilage of adult, pediatric, and microtia sources all exhibited the ability for plastic adherence and colony formation (Figures 1A–1C). Cells from all donors manifested a fibroblast-like morphology with a polygonal and spindle-shaped appearance, which did not change over several passages until passage 5 (Figure S1).

Proliferation rates in each donor group varied per passage. In adult AuCPCs, population doublings per 24 h increased from 0.77 ± 0.07 at passage 1 to 1.49 ± 0.12 at passage 3, after which the rate decreased to 0.58 ± 0.05 doublings at passage 5 (Figure 1D). Pediatric AuCPCs showed a similar trend, starting at 0.43 ± 0.03 doublings per 24 h at passage 1 and peaking at passage 2 with 1.15 ± 0.15 doublings, after which values marginally decreased (Figure 1E). Microtia AuCPCs demonstrated a proliferation rate of 0.49 ± 0.06 doublings per 24 h at passage 1, increasing up to a peak value of 1.24 ± 0.20 during passage 4 (Figure 1F). Differences in proliferation between donor groups were also observed, mainly at passage 3, where adult progenitors exhibited significantly higher population doublings compared to pediatric and microtia groups. Adult-derived cells also exhibited a significantly higher proliferation rate compared to pediatric cells at passage 1. However, at passage 4, both adult and pediatric cells exhibited significantly lower population doublings compared to microtia-derived progenitor cells. Understanding such inter-donor group differences in growth patterns can help establish expansion protocols that take advantage of each cell source's higher cell yields for tissue engineering applications.

Flow cytometry determined the expression of markers typically used to characterize mesenchymal stromal cells (Dominici et al., 2006) in each donor (Figure 2). Of adult AuCPCs, 82.73 ± 4.93% expressed CD90, 92.58 ± 2.53% expressed CD105, and 98.25 ± 1.65% expressed CD73. In pediatric AuCPCs, CD90 was
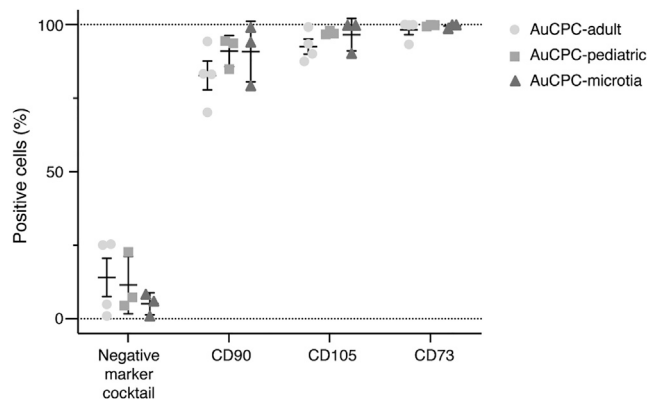
Figure 2. Expression of putative stem cell markers
Using flow cytometry, expression of mesenchymal stromal cell specific markers was measured. Data are represented as mean +/- SEM. Individual data points are also shown. High percentages of cells positive for CD90, CD105, and CD73 were found in adult, pediatric, and microtia populations at passage 4. All populations exhibited a low percentage of expression of a panel of surface markers. This negative marker cocktail consisted of CD11b, CD34, CD45, CD79a, and HLA-DR.

expressed in 91.03 $\pm$ 3.08%, CD105 in 97.20 $\pm$ 0.36%, and CD73 in 99.70 $\pm$ 0.15%. Microtia AuCPCs expressed CD90 in 90.83 $\pm$ 5.94%, CD105 in 96.63 $\pm$ 3.17%, and CD73 in 99.57 $\pm$ 0.43%. Histograms for each group and each marker are presented in Figure S2.

Trilineage differentiation assays confirmed that AuCPC-adult, AuCPC-pediatric, and AuCPC-microtia exhibited *in vitro* multipotency potential over several passages (passage 4 is shown in in Figure 3, and passages 3 and 5 are shown in Figures S3 and S4 respectively). Upon stimulation with the appropriate culture media, an abundant presence of calcifications (Figures 3A–3C), adipose vesicles (Figures 3D–3F), and glycosaminoglycans (Figures 3G–3I) was observed, indicating successful *in vitro* differentiation into the osteogenic, adipogenic, and chondrogenic lineages, respectively. Given these cells' sustained multipotency over multiple passages regardless of their donor source, and each donor group's unique growth pattern, it seems feasible to tailor expansion protocols in a patient-specific manner to ensure that expansion rate and ensuing cell yield are optimal, while ensuring that cells maintain their differentiation capacity.

Differential mRNA expression in hydrogel culture shows chondrogenic marker profile expression

Upon embedding in 3D hydrogel constructs, AuCPCs demonstrated an upregulation of cartilage-specific genes (ACAN, COL2A1, and COMP) after *in vitro* chondrogenic culture. In addition, low expression levels of markers indicating chondrocyte hypertrophy (COL10A1) and osteogenic differentiation (RUNX2) were observed.

Compared to the housekeeping gene HPRT1, aggrecan expression (Figure 4A) increased non-significantly from a 2.99-fold ($\pm$0.78) increment in adult AuCPCs, 12.80-fold ($\pm$8.89) in pediatric AuCPCs, and 7.81-fold ($\pm$4.96) in microtia AuCPCs at day 1 to 27.52-fold ($\pm$4.36), 29.09-fold ($\pm$18.76), and 53.93-fold ($\pm$44.49) at day 56. Similarly, COL2A1 expression (Figure 4B) increased non-significantly from 0.02 ($\pm$0.02), 2.06 ($\pm$2.17), and 0.19 ($\pm$0.30) at day 1 to 19.27 ($\pm$3.64), 28.77 ($\pm$26.21), and 57.11 ($\pm$35.40) at day 56 in adult, pediatric, and microtia AuCPCs, respectively. The expression of COMP (Figure 4C) also increased over time in all groups. A significant increment was observed in adult AuCPCs, rising from a 0.09-fold reduction ($\pm$0.03) at day 1 to a 6.59-fold upregulation ($\pm$1.72) at day 56, and pediatric AuCPCs, showing a similar rise from a 0.22-fold ($\pm$0.14) to a 8.46-fold expression level ($\pm$4.34) after 56 days of culture. Although non-significant, microtia AuCPCs increased their expression from 0.11-fold ($\pm$0.10) at day 1 to 4.35-fold ($\pm$1.55) at day 56.

In all groups, COL10A1 (Figure 4D) was expressed at low levels compared to the housekeeping gene during culture. Its relative fold expression in adult AuCPCs was 0.01 ($\pm$0.003) at day 1 and 0.28 ($\pm$0.09) at day 56, whereas in pediatric AuCPCs there was a 0.04-fold ($\pm$0.03) reduction at both timepoints. Microtia AuCPCs displayed a significant upregulation from a 0.05-fold ($\pm$0.02) at day 1 to a 0.83-fold ($\pm$0.43)

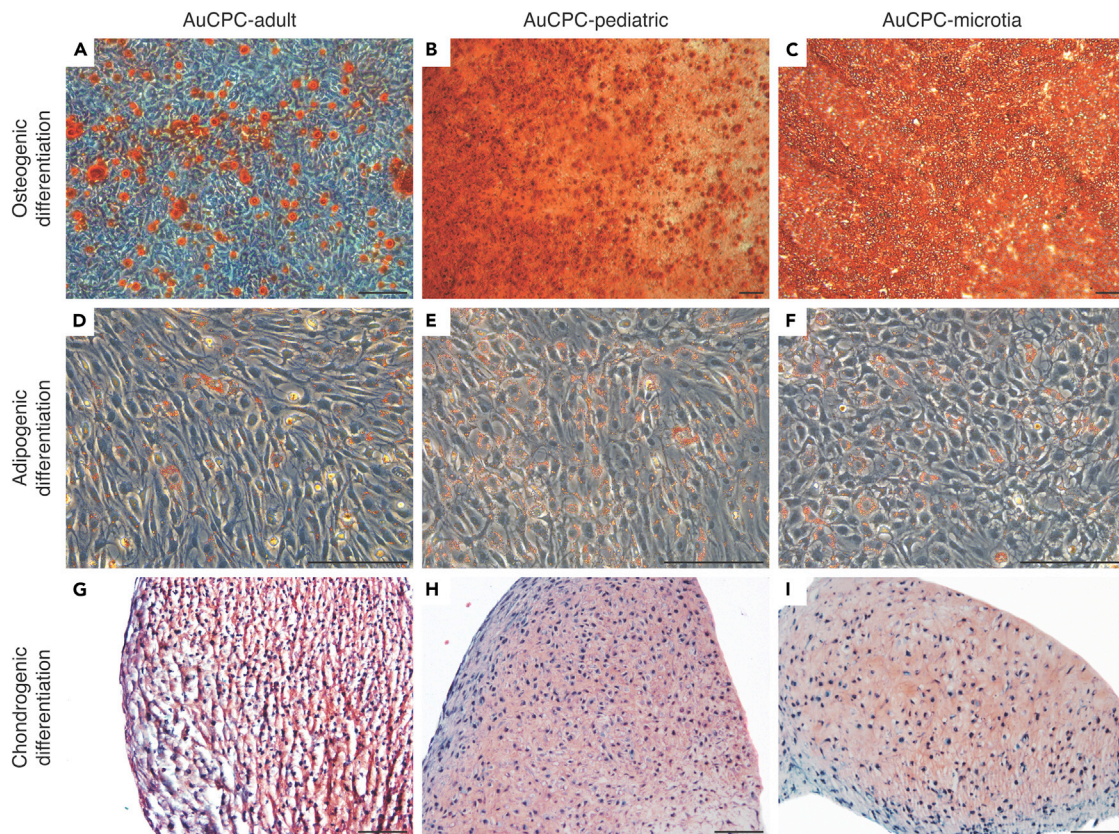AuCPC-adult   AuCPC-pediatric   AuCPC-microtia

Figure 3. Trilineage differentiation capacity in passage 4

AuCPCs sourced from adult, pediatric, and microtia cartilage demonstrated the ability to differentiate toward the osteogenic, adipogenic, and chondrogenic lineages. Upon stimulation with osteogenic culture media, AuCPCs produced mineralizations (A/B/C), whereas in adipogenic culture abundant lipid vesicles were observed (D/E/F). Pelleted cells in chondrogenic differentiation media demonstrated the deposition of glycosaminoglycans (G/H/I). Scale bars represent 100 μm.

reduction, relative to the housekeeping gene, at day 56. This increase in COL10A1 expression was also significantly higher in adult and pediatric AuCPCs.

Osteogenic marker RUNX2 (Figure 4E) levels remained low in all groups. At day 1, the relative fold expression was 0.24 ($\pm$0.05) in adult AuCPCs, 0.24 ($\pm$0.16) in pediatric AuCPCs, and 0.31 ($\pm$0.19) in microtia AuCPCs. Expression increased slightly yet non-significantly over time, with a 0.44-fold ($\pm$0.14), a 0.57-fold ($\pm$0.20), and a 0.48-fold ($\pm$0.28) reduction in adult, pediatric, and microtia AuCPCs, respectively.

Chondrogenic culture of cell-laden hydrogels results in cartilage-specific matrix production

The synthesis of cartilage-specific matrix in cell-laden hydrogel constructs was assessed by the quantification of sulfated glycosaminoglycans (sGAG), which is representative of the proteoglycan content present in the neotissue. All groups demonstrated a significant increase in sGAG per dsDNA content during *in vitro* culture (Figure 5A), confirming chondrogenic differentiation and neocartilage production.

Adult AuCPCs showed a significant increase in sGAG from 1.07 μg/μg ($\pm$0.23) at day 1 to 18.29 μg/μg ($\pm$1.04) at day 28 and 31.52 μg/μg ($\pm$1.44) at day 56. A significant sGAG production was also observed in microtia AuCPCs: 1.03 μg/μg ($\pm$0.09) at day 1, 19.97 μg/μg ($\pm$3.31) at day 28, and 33.23 μg/μg ($\pm$1.84) at day 56 of culture. AuCPCs sourced from pediatric tissue exhibited the highest sGAG values with 0.51 μg/μg ($\pm$0.12) at day 1 significantly increasing to 31.99 μg/μg ($\pm$6.30) at day 28 and then further to 39.51 μg/μg ($\pm$6.93) at day 56. At day 28, their GAG content was significantly higher compared to adult-derived cells.
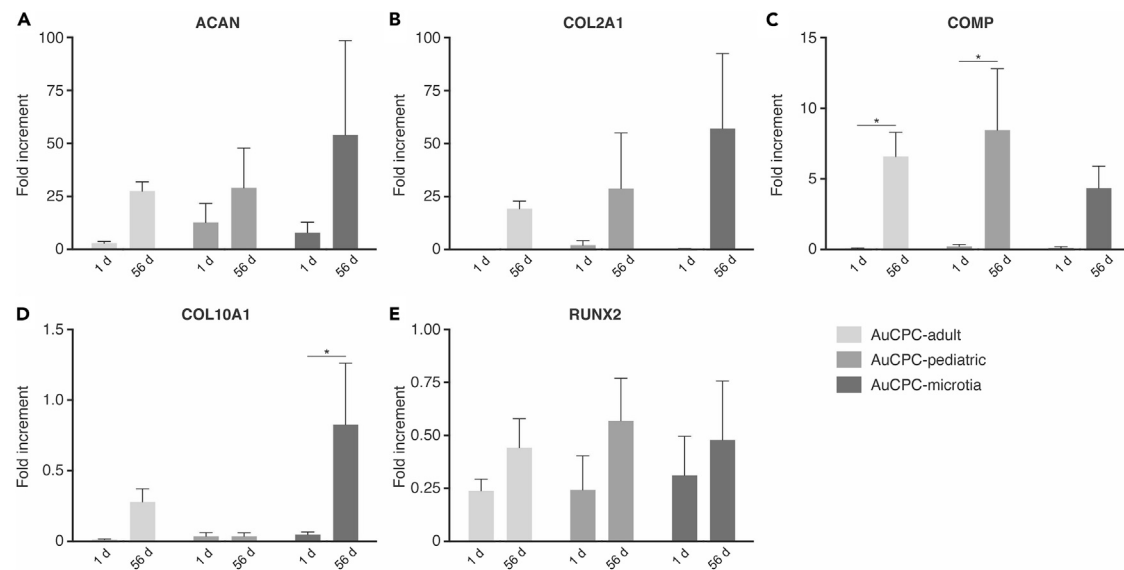
Figure 4. qPCR analysis of chondrogenic marker expression in cell-laden hydrogels

Relative gene expression of (A) aggrecan, (B) collagen type II, (C) cartilage oligomeric matrix protein, (D) collagen type X, and (E) runt-related transcription factor 2, normalized against housekeeping gene HPRT1. Data are represented as mean ± SEM. Analyses were performed through two-way ANOVA with a Bonferroni post-hoc test. Statistically significant differences of $p < 0.05$ are indicated with an asterisk (*).

Hydrogel constructs display increased compressive properties over time

The compression modulus is representative of the stiffness of the cell-laden hydrogel constructs in terms of compression. The modulus increased in all groups during the culture period (Figure 5B).

The compressive Young's modulus significantly increased over time in constructs loaded with adult and pediatric AuCPCs. Adult AuCPC samples exhibited a modulus of 55.09 ± 7.67 kPa at day 28 and 64.82 ± 7.73 kPa at day 56, of which the latter is a significant increase compared to day 1 (40.16 ± 2.87 kPa). Samples with pediatric AuCPCs started at a significantly lower compressive Young's modulus at day 1 (4.25 ± 0.26 kPa) compared to adult AuCPCs and increased significantly at both timepoints (41.15 ± 8.13 kPa at day 28 and 54.19 ± 10.66 kPa at day 56). There was a non-significant increase in compressive strength in microtia AuCPC samples over time, with a modulus of 23.29 ± 2.92 kPa at day 1, 34.00 ± 3.97 kPa at day 28, and 36.62 ± 4.61 kPa at day 56. At this last time point, adult-derived AuCPCs exhibited significantly higher compressive properties compared to microtia-derived cells.

Auricular cartilage-specific matrix deposition is confirmed by histology and immunohistochemistry

The presence and distribution of several components specific for auricular cartilage, including proteoglycans, collagens type II and I, as well as elastin, were visualized on histological sections. The stainings confirm neocartilage matrix deposition in hydrogels loaded with human AuCPCs after *in vitro* culture for up to 56 days.

Synthesized proteoglycans, as indicated by safranin O staining, were most abundant in pediatric AuCPCs, followed by adult AuCPCs. There was an inhomogenous distribution of stained proteoglycans in adult AuCPC samples, with dense labeling in the pericellular territory gradually dispersing into the hydrogel (Figure 6A). Pediatric AuCPCs displayed an intense homogeneous staining throughout the sample, with no observable qualitative increase between day 28 and day 56 (Figure 6B), corresponding to the quantified sGAG content. Microtia AuCPC samples exhibited isolated pericellular staining at day 28, with increasing distribution into the inter-territorial areas at day 56 of culture (Figure 6C).

The deposition of collagen type II and collagen type I was predominantly localized in a broad peripheral area of the hydrogel sample. Collagen type II appeared concentrated pericellularly with clusters of intense brown staining in samples with adult and microtia AuCPCs (Figures 6D and 6F, respectively). Pediatric
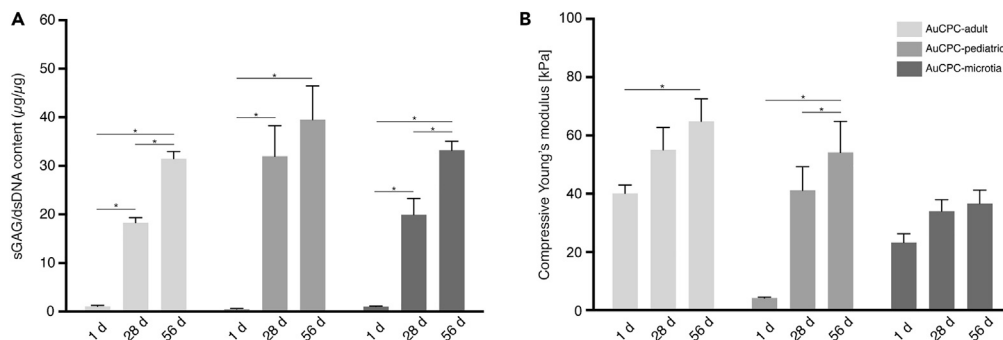
Figure 5. Biochemical composition and compression modulus of cell-laden hydrogels

(A) Quantified sulfated glycosaminoglycan per dsDNA content after 28 and 56 days of chondrogenic culture, normalized against dry weight.

(B) Compressive Young's modulus as a measure of construct stiffness of cell-laden hydrogels after 28 and 56 days of culture. Data are represented as mean ± SEM. Analyses were performed through two-way ANOVA with a Bonferroni post-hoc test. Statistically significant differences of $p < 0.05$ are indicated with an asterisk (*).

AuCPCs displayed less intense staining, yet with a more widely distributed organization of collagens into the inter-territorial region, with a more intense staining observed pericellularly (Figure 6E). At day 56, microtia AuCPCs displayed the most intense collagen type II staining, corresponding to the mRNA expression profiles. Staining for collagen type I was generally less pronounced compared to collagen type II (Figures 6G–6I). In all groups, staining remained localized in a wide territorial area and intensified slightly over time.

Elastin is a specific component of elastic auricular cartilage. All groups displayed a weak intracellular staining for elastin (Figures 6J and 6K). Staining was most apparent in samples containing pediatric AuCPCs, followed by microtia and adult AuCPCs.

DISCUSSION

The origin of the cells used for the generation of elastic cartilage-like tissue is an essential factor in determining the success of tissue-engineered auricular implants. However, the limitations of currently used cell sources—including chondrocytes and MSCs—hamper the development of high-quality engineered tissue constructs. Cartilage progenitor cells (CPC) are a new player in cartilage tissue engineering that, due to their high proliferative potential and dedicated chondrogenic differentiation capacity, require only a small biopsy to generate sufficient cells for the generation of a cartilage structure of clinically relevant sizes. In addition, CPCs from equine sources have previously been shown to generate high-quality neocartilage in an *in vitro* hydrogel model (Otto et al., 2018; Levato et al., 2017). This study is the first to identify fibronectin-adhering human auricular cartilage progenitor cells in adult and pediatric cartilage and confirm their potency for cartilage tissue engineering applications. Importantly, in pediatric tissues, these cells have been identified and isolated also from rudimentary microtia auricular cartilage, showing for the first time, how even in this underdeveloped cartilage remnant there still exists a multipotent progenitor cell population with the potential to generate physiological-like chondral tissue. This novel human cell source has the potential to improve the quality and clinical feasibility of autologous tissue-engineered auricular implants, facilitate the successful translation of the technology toward the clinic, and thus advance microtia reconstruction toward a less invasive technique. However, given the limited study of such underdeveloped tissue as a tissue engineering cell source and some differences observed in their growth and differentiation profiles compared to healthy donor sources, further study is essential to establish their safety and efficiency for clinical applications.

The engineering of a human-sized auricle would require between 100 and 250 million cells, depending on implant volume and seeding density (Bichara et al., 2012; Cohen et al., 2018; Bernstein et al., 2018). Chondrocytes maintain a low proliferative capacity and are known to dedifferentiate in monolayer culture due to continuous multiplication, passaging, and low seeding densities, shifting toward a fibroblast-like phenotype and corresponding matrix production that is lacking the biochemical and biomechanical properties of native elastic cartilage (Bichara et al., 2012; Schnabel et al., 2002; Homicz et al., 2002; Mandl et al.,
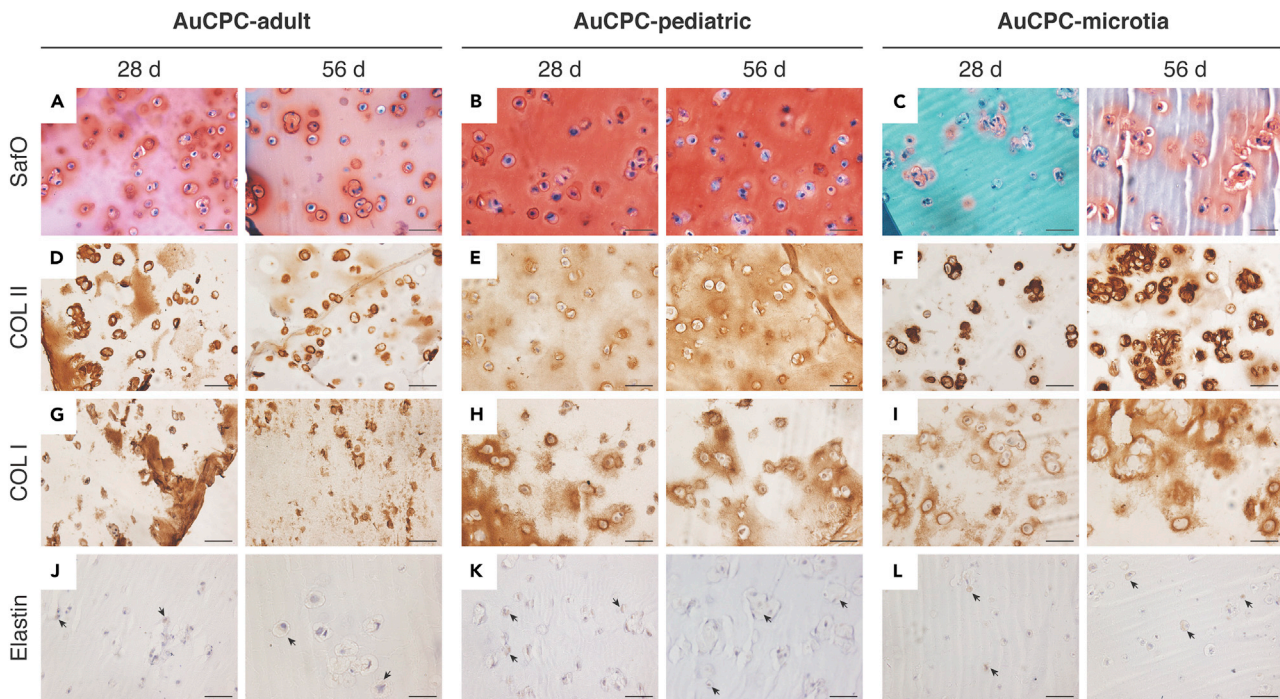
Figure 6. Histological analysis of cell-laden hydrogels after 28 and 56 days in chondrogenic culture
Safranin O staining visualizing proteoglycan deposition in (A) adult, (B) pediatric, and (C) microtia AuCPCs. Immunohistochemistry for (D/E/F) collagen type II, (G/H/I) collagen type I, and (J/K/L) elastin. Black arrows indicate places of intracellular elastin staining. Scale bars represent 50 μm.

2004; Chung et al., 2006; Schulze-Tanzil et al., 2004; Lee et al., 2007; Nabzdyk et al., 2009). Approximately 2 million chondrocytes can be harvested from a non-deforming biopsy from the human auricle (Mandl et al., 2004), which can only be expanded to roughly 10 million cells before undesirable phenotypic changes occur (Bernstein et al., 2018). Cartilage progenitor cells, on the other hand, have stem-cell like properties and can be readily expanded to high cell numbers while maintaining chondrogenic differentiation capacity in an inducive environment. The CPC subpopulation comprises 0.1%–1% of the total cell content of cartilage (Williams et al., 2010; Dowthwaite et al., 2004). Auricular CPCs can be easily obtained from the rudimentary cartilage in microtia or through a non-deforming biopsy from the normal external ear. This would yield between 2 and 20 thousand AuCPCs, which can then be expanded and passaged multiple times, generating over 250 million cells in only 11 to 17 population doublings. Following our results on the proliferation capacity of human AuCPCs, with growth rates ranging from 0.43 to 1.49 population doublings per 24 h, these cell numbers could be attainable within one to six weeks of *in vitro* culture and in less than 5 passages. During this time, AuCPCs do not lose their capacity for multi-lineage differentiation. This study demonstrated the ability of AuCPCs to differentiate toward osteoblasts, adipocytes, and chondrocytes after 3, 4, and 5 passages. Chondrogenic matrix deposition remained abundant among donor sources and over time; only adult AuCPCs, which were sourced from elderly donors, displayed diminished cartilage production at passage 5.

Distinctive properties of CPCs include their ability to form large colonies from an initially low seeding density (Dowthwaite et al., 2004), the expression of the putative stem cell markers CD73, CD90, and CD105 (Williams et al., 2010; Dominici et al., 2006) as well as the fibronectin receptor CD49e (Williams et al., 2010), and the retainment of multi-lineage differentiation potential (Williams et al., 2010). These factors discern this specific subpopulation of cartilage-resident stem/progenitor cells from other cell samples that are frequently named chondroprogenitors—a term often used for any progenitor cell driven toward the chondrogenic lineage (Jayasuriya and Chen, 2015). In accordance with the standard definition for MSCs (Dominici et al., 2006), AuCPCs are plastic adherent and demonstrate the potential to differentiate into multiple lineages. Furthermore, ≥95% of the putative stem cell population must express surface antigens specific to CD90, CD105, and CD73, which partially applies to the AuCPCs found in our study. Given our analysis, human AuCPCs qualify in terms of CD105 and CD73 expression but defer from the standard

definition of MSCs in the case of CD90 expression. However, this set of markers has been specifically developed to distinguish MSCs from other stem cell types (*i.e.* hematopoietic stem cells in the bone marrow) and may not fully match the profile of other mesenchymal progenitor cells present in different tissues. To date, there is no unique set of markers identified for the selection of CPCs derived from articular cartilage (the most studied source of chondroprogenitors), and even less is known about auricular cartilage-resident progenitor cells (Xue et al., 2016; Otto et al., 2018; Zhang et al., 2019). Some preliminary studies are starting to indicate potential markers to distinguish articular chondroprogenitors, such as co-expression of CD166 and STRO-1 (Alsalameh et al., 2004; Vinod et al., 2017), which may be useful for auricular progenitors as well. Regardless, plastic adherence, colony formation, abundant proliferative abilities, and multipotent differentiation capacity are stem cell-associated properties that are highly beneficial for tissue engineering purposes. AuCPCs are therefore an interesting alternative cell source for bioengineering-based auricular reconstruction.

Besides a potent cell source, successful cartilage tissue engineering requires an appropriate microenvironment for maturing cells to thrive in. Specifically, a three-dimensional (3D) environment is a key element in supporting the chondrogenic potential of cells, thereby fostering a cartilage-like gene expression profile and corresponding extracellular matrix production (Pampaloni et al., 2007). Hydrogels are especially suitable as cell carriers, being highly hydrated porous polymer networks that can provide a permissive 3D environment for chondrogenic differentiation and neocartilage formation (Vega et al., 2017). Gelatin methacryloyl (GelMA) has proven to be a favorable choice for cartilage tissue engineering strategies due to its biocompatibility, natural bioactivity, and tailorability (Klotz et al., 2016). This hydrogel system has previously been shown to be conducive for chondrogenesis (Levato et al., 2017; Levett et al., 2013; Schuurman et al., 2013) and to support equine auricular and articular CPCs in producing cartilage-like matrix *in vitro* (Otto et al., 2018; Levato et al., 2017). Similarly, the human AuCPCs in this study demonstrated evident chondrogenic potential in GelMA constructs. At the genetic level, the differential expression of markers for aggrecan, collagen type II, and cartilage oligomeric matrix protein all increased over the 56-day culture period. Biochemical analysis confirmed the synthesis of cartilage-like matrix in hydrogels seeded with AuCPCs.

Proteoglycans are the major structural components of cartilage. The quantification of glycosaminoglycans showed a significant increase of GAG per DNA over time in all groups, indicating abundant neotissue matrix synthesis. The conglomeration of proteoglycans contributes to the mechanical properties of cartilage tissue. Corresponding with the biochemical results, a significant increase in compressive modulus over time was found in samples laden with adult and pediatric AuCPCs; however, this was not the case for microtia AuCPCs. Histological evaluation may provide an explanation for this observation. Cartilage-specific matrix deposition in cell-laden hydrogels was evident in all constructs laden with adult, pediatric, or microtia AuCPCs. Nevertheless, pediatric AuCPCs exhibited a homogeneous distribution of synthesized matrix components throughout the hydrogel, whereas the deposition of proteoglycans and collagens by microtia AuCPCs remained predominantly in the pericellular to territorial matrices. As the specific organization of a tissue impacts its mechanical properties (Wu and Herzog, 2002), the non-significant changes in compressive modulus in constructs with microtia cells, which differ significantly from adult-derived cells after 56 days, may be attributed to this inhomogeneous cluster-like organization. In contrast, the more homogeneous incorporation of proteoglycans in the extracellular matrix by adult and pediatric AuCPCs appears to contribute significantly to the increasing compressive properties of the constructs. The compression moduli achieved in this study by encapsulating human AuCPCs in gelMA, ranging from 36.6 to 64.8 kPa after 56 days of culture, are markedly lower than the native situation. Various biomechanical properties of native auricular cartilage have been reported to be at least in the MPa range (Griffin et al., 2016; Nimeskern et al., 2015), demanding tissue-engineered constructs to be structurally enhanced with supporting frames (Cervantes et al., 2013; Visscher et al., 2019) or with a more refined reinforcing fiber network (Visser et al., 2015; Melchels et al., 2016; Kang et al., 2016). Such strategies can mechanically support engineered constructs during *in vitro* and *in vivo* maturation of the neotissue.

Specific to auricular cartilage is the presence of a network of elastin fibers. Elastin is critical for the long-term function of the auricular cartilage and the maintenance of its shape, as this biopolymer is stable, durable, and allows elastic recoil and resilience of the tissue (Mithieux and Weiss, 2005). The development of elastic fibers is slower compared to other cartilage matrix components (Cohen et al., 2018). In studies applying auricular chondrocytes or a chondrocyte-MSC co-culture in a pellet or hydrogel system, elastin fibers started appearing after 6–12 weeks of *in vivo* culture (Cohen et al., 2018; Bichara et al., 2014;

Bernstein et al., 2018; Cai et al., 2015; Hellingman et al., 2011; van Osch et al., 2004). Although the specific requirements for elastin formation are still largely uncertain, it has been suggested that *in vitro* culture alone is insufficient (Hellingman et al., 2011). In a study by Hellingman et al. (2011), an absence of elastin was observed after 10 weeks *in vitro* culture of pelleted auricular chondrocytes, whereas implanted samples demonstrated elastin production after 6 weeks *in vivo*. Our study showed a weak intracellular expression of elastin by AuCPCs, as indicated by immunohistochemical staining, after 8 weeks of *in vitro* culture in GelMA. These preliminary results could indicate the early development of elastin fibers. The supplementation of the differentiation media with TGF-β1, known for its ability to stimulate the expression of tropoelastin (Mithieux and Weiss, 2005), may be a contributing factor to this observation. Another explanation may be the inherent potency of AuCPCs to reproduce their native environment, *i.e.* the elastic cartilage of the auricle. Nevertheless, the expression and deposition of elastin fibers by AuCPCs should be further assessed on a longer time frame.

The bending properties of the ear are integral for withstanding the daily external influences on the auricular structure. Hence, stimulating the formation of elastic fibers in tissue-engineered cartilage for the auricle is necessary, yet the importance of preventing the formation of calcifications should not be overlooked. Cartilage calcifications after auricular reconstruction are undesirable as mineralization of the neotissue can lead to loss of flexibility, increased stiffness, an unnatural feel of the reconstructed ear, patient discomfort, shape distortion, and potential risk of implant fracture or extrusion through the skin (Bichara et al., 2012; Jessop et al., 2016; Nimeskern et al., 2014; Kim et al., 2019). As such, avoidance of cellular hypertrophy and subsequent tissue mineralization is essential. A marker of chondrocyte hypertrophy is collagen type X (Martin et al., 2001), whereas RUNX2 is a marker of osteogenic differentiation (Komori, 2006). Collagen type X is actually present in native non-mineralized auricular cartilage (Pappa et al., 2013; Hellingman et al., 2011; Dahl et al., 2011; Giardini-Rosa et al., 2014) and its expression without subsequent mineralization has been reported in several studies applying chondrocytes for cartilage tissue engineering (Hellingman et al., 2011; Dahl et al., 2011). In our study, the mRNA expression of collagen type X was low in adult and pediatric AuCPCs; however, its expression was significantly upregulated in microtia AuCPCs after the 56-day culture period. In addition, a non-significant upregulation of RUNX2 was observed in all groups during the 8-week culture period. Compared to markers more typical of mature cartilage, *i.e.* aggrecan, collagen type II, and cartilage oligomeric matrix protein, the expression levels of COL10A1 and RUNX2 are very low. Our previous study using equine AuCPCs showed similar expression levels of these markers without mineralization of the neotissue, as confirmed by histology (Otto et al., 2018). Nevertheless, given the significant COL10A1 upregulation in microtia-derived cells, maintenance of the chondrogenic phenotype should be monitored for human AuCPCs in future studies, during long-term *in vitro* culture and even more so during *in vivo* application.

As microtia is a developmental disorder associated with genetic aberrations (Luquetti et al., 2012), cells sourced from rudimentary microtia cartilage may have different properties than those from normal cartilage. Microtia cartilage has a more disorganized microscopic appearance, yet gene expression profiles and biochemical composition are similar to normal auricular cartilage (Ishak et al., 2011; Melgarejo-Ramírez et al., 2016; Gu et al., 2017). There are only a few studies that have compared microtia chondrocytes to healthy human chondrocytes when applied for tissue engineering purposes, and although the majority found them to synthesize similar neocartilage tissue *in vivo* (Ishak et al., 2011, 2015; Kamil et al., 2004; Nakao et al., 2017), contrasting results have been reported. A recent comparison describes higher GAG content, higher Young's modulus, and higher cartilage-specific gene expression by healthy chondrocytes (Gu et al., 2017). Our study is the first to report on cartilage progenitor cells sourced from the rudimentary microtia cartilage and our results indicate the ability of these cells to synthesize new cartilage tissue in an *in vitro* 3D hydrogel system. Compared to healthy adult and pediatric AuCPCs, cells from microtia cartilage seem to perform somewhat differently in terms of matrix organization and gene expression levels. Their aberrant origin and performance remains a point of further investigation, focusing on genetic profiles and regenerative behavior in the long-term. Nevertheless, the rudimentary microtia cartilage can be a very valuable source of potent cartilage-producing cells, obviating the need for biopsies in healthy tissues.

Another important observation in this study is the variability between individual donors. This is a well-known challenge in cells and tissues originating from human sources (Stoddart et al., 2012). When evaluating group averages, donor variance can be reflected in the SD, yet this may impair the statistical analysis when comparing different groups. For improved insight in the regenerative response, it may be useful to correlate the results of each donor individually. Although in our study most donors exhibited substantial

regenerative potential, we found some donors to underperform, thereby affecting average group results and statistical outcomes. Donor-to-donor variance may be linked to age, gender, and disease (Siegel et al., 2013; Strässler et al., 2018). Nevertheless, our results show that even in case of microtia, potent and regeneration-competent cells are residing in the tissue. It would be advisable to start assessing individual donor performance and to subsequently determine the factors that can predict satisfactory outcomes. In the end, personalized medicine ultimately requires the definition of a set of quality control markers to benchmark whether the harvested cells are good enough to use for tissue engineering applications for that patient.

Surgical correction of auricular deformities can greatly enhance a patient's psychosocial functioning and quality of life. The current state-of-the-art treatments bring meaningful change, yet have donor site morbidities, absence of a natural feel, and in case of foreign material the chance of implant extrusion. Therefore, improved reconstruction strategies are desired. The tissue engineering approach using autologous cells and bioresorbable supporting materials could provide a long-term solution, by essentially regenerating native-like tissue with appropriate properties. Challenges remain in obtaining sufficient autologous cells and subsequently generating high-quality neotissue. Auricular cartilage progenitor cells have the ability to supply the required cell numbers for tissue engineering of an auricular implant, while maintaining the chondrogenic phenotype and producing cartilage-like neotissue in a 3D hydrogel system. These cells can be easily obtained through a non-deforming biopsy of the normal ear or from the rudimentary microtia cartilage. As such, the availability of a potent progenitor subpopulation in the human auricular cartilage presents encouraging opportunities for the successful engineering of the human auricle and its translation toward the clinic.

Limitations of the study

A well-known challenge in studies using cells and materials from human sources is the marked variability between individual donors. This was also observed in our study, and this donor-to-donor variability can cloud the identification of specific differences in certain performance indicators, especially when small numbers of donors are used. Thus, while the current work provides for the first time a key insight on the presence of human AuCPCs, it is advisable to screen larger numbers of donor. Importantly, identifying reliable biomarkers that can be used as predictors of the performance of a specific donor remains a major unsolved challenge in the field, and will be needed to expedite the clinical translation of cell-based regenerative therapies.

The neosynthesis of elastin fibers within engineered tissue is an important outcome of successful cartilage regeneration for the human auricle. In our study, we found a weak intracellular presence of elastin produced by AuCPCs, as indicated by immunohistochemical staining, which could indicate the early development of elastin fibers. While optimal culture conditions to enhance elastin production and secretion are still being investigated, the application of dynamic mechanical loads, which were not included in this study, can be beneficial, as already shown for other cell types (Takebe et al., 2012). Overall, our data provide important insights on a recently identified human auricular chondroprogenitor cell subset that can be even retrieved from clinically relevant autologous sources like microtic redundant tissue. Further long-term *in vitro*, as well as *in vivo* studies will be required to evaluate the elastin production potential of auricular cartilage progenitor cells, and their ability to be used as components in therapies to restore damaged auricles.

STAR★METHODS

Detailed methods are provided in the online version of this paper and include the following:

- KEY RESOURCES TABLE
- RESOURCE AVAILABILITY
  - Lead contact
  - Materials availability
  - Data and code availability
- EXPERIMENTAL MODEL AND SUBJECT DETAILS
  - Human auricular cartilage
  - Isolation of cartilage progenitor cells
- METHOD DETAILS
  - Visualization of cell morphology

- ○ Evaluation of growth rates
- ○ Stem cell marker expression
- ○ Assessment of multipotency
- ○ Fabrication of 3D cell-laden hydrogel constructs
- ○ Gene expression of cartilage markers
- ○ Biochemical analysis of cell-laden hydrogels
- ○ Compressive mechanical testing
- ○ Histology and immunohistochemistry
- ● QUANTIFICATION AND STATISTICAL ANALYSIS

SUPPLEMENTAL INFORMATION

Supplemental information can be found online at https://doi.org/10.1016/j.isci.2022.104979.

AUTHOR CONTRIBUTIONS

Conceptualization by I.A.O., M.K., C.C.B., R.L., and J.M.; Methodology by I.A.O. and R.L.; Investigation by I.A.O., P.N.B., M.R., M.H.P.R., and A.M.; Formal Analysis by I.A.O., P.N.B., and M.R.; Writing of the original draft by I.A.O.; Review & Editing by I.A.O., P.N.B., R.L., and J.M.; Resources & Visualization by I.A.O. and P.N.B.; Project Administration by I.A.O.; Supervision by M.K., C.C.B., R.L., and J.M.

DECLARATION OF INTERESTS

The authors declare no competing interests.

REFERENCES

Alasti, F., and Van Camp, G. (2009). Genetics of microtia and associated syndromes. J. Med. Genet. 46, 361–369.

Alsalameh, S., Amin, R., Gemba, T., and Lotz, M. (2004). Identification of mesenchymal progenitor cells in normal and osteoarthritic human articular cartilage. Arthritis Rheum. 50, 1522–1532.

Baluch, N., Nagata, S., Park, C., Wilkes, G.H., Reinisch, J., Kasrai, L., and Fisher, D. (2014). Auricular reconstruction for microtia: a review of available methods. Plast. Surg. 22, 39–43.

Bauer, B.S. (2009). Reconstruction of microtia. Plast. Reconstr. Surg. 124, 14e–26e.

Bernstein, J.L., Cohen, B.P., Lin, A., Harper, A., Bonassar, L.J., and Spector, J.A. (2018). Tissue engineering auricular cartilage using late passage human auricular chondrocytes. Ann. Plast. Surg. 80, S168–S173.

Bichara, D.A., O'Sullivan, N.-A., Pomerantseva, I., Zhao, X., Sundback, C.A., Vacanti, J.P., and Randolph, M.A. (2012). The tissue-engineered auricle: past, present, and future. Tissue Eng. Part B Rev. 18 (1), 51–61.

Bichara, D.A., Pomerantseva, I., Zhao, X., Zhou, L., Kulig, K.M., Tseng, A., Kimura, A.M., Johnson, M.A., Vacanti, J.P., Randolph, M.A., and Sundback, C.A. (2014). Successful creation of tissue-engineered autologous auricular cartilage

in an immunocompetent large animal model. Tissue Eng. Part A 20, 303–312.

Cai, Z., Pan, B., Jiang, H., and Zhang, L. (2015). Chondrogenesis of human adipose-derived stem cells by in vivo co-graft with auricular chondrocytes from microtia. Aesthetic Plast. Surg. 39, 431–439.

Cenzi, R., Farina, A., Zuccarino, L., and Carinci, F. (2005). Clinical outcome of 285 Medpor grafts used for craniofacial reconstruction. J. Craniofac. Surg. 16, 526–530.

Cervantes, T.M., Bassett, E.K., Tseng, A., Kimura, A., Roscioli, N., Randolph, M.A., Vacanti, J.P., Hadlock, T.A., Gupta, R., Pomerantseva, I., and Sundback, C.A. (2013). Design of composite

scaffolds and three-dimensional shape analysis for tissue-engineered ear. J. R. Soc. Interface 10, 20130413.

Chung, C., Mesa, J., Miller, G.J., Randolph, M.A., Gill, T.J., and Burdick, J.A. (2006). Effects of auricular chondrocyte expansion on neocartilage formation in photocrosslinked hyaluronic acid networks. Tissue Eng. 12, 2665–2673.

Ciorba, A., and Martini, A. (2006). Tissue engineering and cartilage regeneration for auricular reconstruction. Int. J. Pediatr. Otorhinolaryngol. 70, 1507–1515.

Cohen, B.P., Bernstein, J.L., Morrison, K.A., Spector, J.A., and Bonassar, L.J. (2018). Tissue engineering the human auricle by auricular chondrocyte-mesenchymal stem cell co-implantation. PLoS One 13, e0202356.

Czekanska, E.M. (2011). Assessment of cell proliferation with resazurin-based fluorescent dye. Methods Mol. Biol. 740, 27–32.

Dahl, J.P., Caballero, M., Pappa, A.K., Madan, G., Shockley, W.W., and van Aalst, J.A. (2011). Analysis of human auricular cartilage to guide tissue-engineered nanofiber-based chondrogenesis: implications for microtia reconstruction. Otolaryngol. Head Neck Surg. 145, 915–923.

Dominici, M., Le Blanc, K., Mueller, I., Slaper-Cortenbach, I., Marini, F., Krause, D., Deans, R., Keating, A., Prockop, D., and Horwitz, E. (2006). Minimal criteria for defining multipotent mesenchymal stromal cells. The International Society for Cellular Therapy position statement. Cytotherapy 8, 315–317.

Dowthwaite, G.P., Bishop, J.C., Redman, S.N., Khan, I.M., Rooney, P., Evans, D.J.R., Haughton, L., Bayram, Z., Boyer, S., Thomson, B., et al. (2004). The surface of articular cartilage contains a progenitor cell population. J. Cell Sci. 117, 889–897.

Gardner, O.F.W., Archer, C.W., Alini, M., and Stoddart, M.J. (2013). Chondrogenesis of mesenchymal stem cells for cartilage tissue engineering. Histol. Histopathol. 28, 23–42.

Gawlitta, D., Farrell, E., Malda, J., Creemers, L.B., Alblas, J., and Dhert, W.J.A. (2010). Modulating endochondral ossification of multipotent stromal cells for bone regeneration. Tissue Eng. Part B Rev. 16, 385–395.

Giardini-Rosa, R., Joazeiro, P.P., Thomas, K., Collavino, K., Weber, J., and Waldman, S.D. (2014). Development of scaffold-free elastic cartilaginous constructs with structural similarities to auricular cartilage. Tissue Eng. Part A 20, 1012–1026.

Griffin, M.F., Premakumar, Y., Seifalian, A.M., Szarko, M., and Butler, P.E.M. (2016). Biomechanical characterisation of the human auricular cartilages; implications for tissue engineering. Ann. Biomed. Eng. 44, 3460–3467.

Gu, Y., Kang, N., Dong, P., Liu, X., Wang, Q., Fu, X., Yan, L., Jiang, H., Cao, Y., and Xiao, R. (2017). Chondrocytes from congenital microtia possess an inferior capacity for in vivo cartilage regeneration to healthy ear chondrocytes. J. Tissue Eng. Regen. Med. 12, e1737–e1746.

Hellingman, C.A., Verwiel, E.T.P., Slagt, I., Koevoet, W., Poublon, R.M.L., Nolst-Trenité, G.J., Baatenburg de Jong, R.J., Jahr, H., and van Osch, G.J.V.M. (2011). Differences in cartilage-forming capacity of expanded human chondrocytes from ear and nose and their gene expression profiles. Cell Transplant. 20, 925–940.

Homicz, M.R., Schumacher, B.L., Sah, R.L., and Watson, D. (2002). Effects of serial expansion of septal chondrocytes on tissue-engineered neocartilage composition. Otolaryngol. Head. Neck Surg. 127, 398–408.

Horlock, N., Vögelin, E., Bradbury, E.T., Grobbelaar, A.O., and Gault, D.T. (2005). Psychosocial outcome of patients after ear reconstruction: a retrospective study of 62 patients. Ann. Plast. Surg. 54, 517–524.

Hurley, D.J., Arbab-Zavar, B., and Nixon, M.S. (2008). The ear as a biometric. In Handbook of Biometrics, A.K. Jain, P. Flynn, and A.A. Ross, eds. (Boston: Springer), pp. 131–150.

Ishak, M.F., Chua, K.H., Asma, A., Saim, L., Aminuddin, B.S., Ruszymah, B.H.I., and Goh, B.S. (2011). Stem cell genes are poorly expressed in chondrocytes from microtic cartilage. Int. J. Pediatr. Otorhinolaryngol. 75, 835–840.

Ishak, M.F.B., See, G.B., Hui, C.K., Abdullah, A.B., Saim, L.B., Saim, A.B., et al. (2015). The formation of human auricular cartilage from microtic tissue: An in vivo study. Int. J. Pediatr. Otorhinolaryngol. 79, 1634–1639.

Jayasuriya, C.T., and Chen, Q. (2015). Potential benefits and limitations of utilizing chondroprogenitors in cell-based cartilage therapy. Connect. Tissue Res. 56, 265–271.

Jessop, Z.M., Javed, M., Otto, I.A., Combellack, E.J., Morgan, S., Breugem, C.C., Archer, C.W., Khan, I.M., Lineaweaver, W.C., Kon, M., et al. (2016). Combining regenerative medicine strategies to provide durable reconstructive options: auricular cartilage tissue engineering. Stem Cell Res. Ther. 7, 19.

Jessop, Z.M., Al-Sabah, A., Simoes, I.N., Burnell, S.E.A., Pieper, I.L., Thornton, C.A., Whitaker, I.S., Simoes, I.N., Burnell, S.E.A., Pieper, I.L., et al. (2020). Isolation and characterisation of nasoseptal cartilage stem/progenitor cells and their role in the chondrogenic niche. Stem Cell Res. Ther. 11, 177.

Johns, A.L., Lucash, R.E., Im, D.D., and Lewin, S.L. (2015). Pre and post-operative psychological functioning in younger and older children with microtia. J. Plast. Reconstr. Aesthet. Surg. 68, 492–497.

Kamil, S.H., Kojima, K., Vacanti, M.P., Bonassar, L.J., Vacanti, C.A., and Eavey, R.D. (2003). In vitro tissue engineering to generate a human-sized auricle and nasal tip. Laryngoscope 113, 90–94.

Kamil, S.H., Vacanti, M.P., Vacanti, C.A., and Eavey, R.D. (2004). Microtia chondrocytes as a donor source for tissue-engineered cartilage. Laryngoscope 114, 2187–2190.

Kang, N., Liu, X., Guan, Y., Wang, J., Gong, F., Yang, X., Yan, L., Wang, Q., Fu, X., Cao, Y., and Xiao, R. (2012). Effects of co-culturing BMSCs and auricular chondrocytes on the elastic modulus

and hypertrophy of tissue engineered cartilage. Biomaterials 33, 4535–4544.

Kang, H.-W., Lee, S.J., Ko, I.K., Kengla, C., Yoo, J.J., and Atala, A. (2016). A 3D bioprinting system to produce human-scale tissue constructs with structural integrity. Nat. Biotechnol. 34, 312–319.

Kim, H.Y., Jung, S.Y., Lee, S.J., Lee, H.J., Truong, M.-D., and Kim, H.S. (2019). Fabrication and characterization of 3D-printed elastic auricular scaffolds: a pilot study. Laryngoscope 129, 351–357.

Klotz, B.J., Gawlitta, D., Rosenberg, A.J.W.P., Malda, J., and Melchels, F.P.W. (2016). Gelatin-methacryloyl hydrogels: towards biofabrication-based tissue repair. Trends Biotechnol. 34, 394–407.

Komori, T. (2006). Regulation of osteoblast differentiation by transcription factors. J. Cell. Biochem. 99, 1233–1239.

Kuo, C.K., Li, W.-J., Mauck, R.L., and Tuan, R.S. (2006). Cartilage tissue engineering: its potential and uses. Curr. Opin. Rheumatol. 18, 64–73.

Kusuhara, H., Isogai, N., Enjo, M., Otani, H., Ikada, Y., Jacquet, R., Lowder, E., and Landis, W.J. (2008). Tissue engineering a model for the human ear: assessment of size, shape, morphology, and gene expression following seeding of different chondrocytes. Wound Repair Regen. 17, 136–146.

Langer, R., and Vacanti, J.P. (1993). Tissue engineering. Science 260, 920–926.

Lee, J., Lee, E., Kim, H.-Y., and Son, Y. (2007). Comparison of articular cartilage with costal cartilage in initial cell yield, degree of dedifferentiation during expansion and redifferentiation capacity. Biotechnol. Appl. Biochem. 48 (Pt 3), 149–158.

Levato, R., Webb, W.R., Otto, I.A., Mensinga, A., Zhang, Y., van Rijen, M., van Weeren, R., Khan, I.M., and Malda, J. (2017). The bio in the ink: cartilage regeneration with bioprintable hydrogels and articular cartilage-derived progenitor cells. Acta Biomater. 61, 41–53.

Levett, P.A., Melchels, F.P.W., Schrobback, K., Hutmacher, D.W., Malda, J., and Klein, T.J. (2013). A biomimetic extracellular matrix for cartilage tissue engineering centered on photocurable gelatin, hyaluronic acid and chondroitin sulfate. Acta Biomater. 10, 214–223.

Liu, X., Sun, H., Yan, D., Zhang, L., Lv, X., Liu, T., Zhang, W., Liu, W., Cao, Y., and Zhou, G. (2010). In vivo ectopic chondrogenesis of BMSCs directed by mature chondrocytes. Biomaterials 31, 9406–9414.

Luquetti, D.V., Heike, C.L., Hing, A.V., Cunningham, M.L., and Cox, T.C. (2012). Microtia: epidemiology and genetics. Am. J. Med. Genet. A 158A, 124–139.

Magritz, R., and Siegert, R. (2014). Auricular reconstruction: surgical innovations, training methods, and an attempt for a look forward. Facial Plast. Surg. 30, 183–193.

Mandl, E.W., van der Veen, S.W., Verhaar, J.A.N., and van Osch, G.J.V.M. (2002). Serum-free medium supplemented with high-concentration

FGF2 for cell expansion culture of human ear chondrocytes promotes redifferentiation capacity. Tissue Eng. 8, 573–580.

Mandl, E.W., Jahr, H., Koevoet, J.L.M., van Leeuwen, J.P.T.M., Weinans, H., Verhaar, J.A.N., and van Osch, G.J.V.M. (2004). Fibroblast growth factor-2 in serum-free medium is a potent mitogen and reduces dedifferentiation of human ear chondrocytes in monolayer culture. Matrix Biol. 23, 231–241.

Martin, I., Jakob, M., Schäfer, D., Dick, W., Spagnoli, G., and Heberer, M. (2001). Quantitative analysis of gene expression in human articular cartilage from normal and osteoarthritic joints. Osteoarthritis Cartilage 9, 112–118.

Melchels, F.P.W., Dhert, W.J.A., Hutmacher, D.W., and Malda, J. (2014). Development and characterisation of a new bioink for additive tissue manufacturing. J. Mater. Chem. B 2, 2282–2289.

Melchels, F.P.W., Blokzijl, M.M., Levato, R., Peiffer, Q.C., de Ruijter, M., Hennink, W.E., Vermonden, T., and Malda, J. (2016). Hydrogel-based reinforcement of 3D bioprinted constructs. Biofabrication 8, 035004.

Melgarejo-Ramírez, Y., Sánchez-Sánchez, R., García-López, J., Brena-Molina, A.M., Gutiérrez-Gómez, C., Ibarra, C., and Velasquillo, C. (2016). Characterization of pediatric microtia cartilage: a reservoir of chondrocytes for auricular reconstruction using tissue engineering strategies. Cell Tissue Bank. 17, 481–489.

Mithieux, S.M., and Weiss, A.S. (2005). Elastin. Adv. Protein Chem. 70, 437–461.

Mueller, M.B., and Tuan, R.S. (2008). Functional characterization of hypertrophy in chondrogenesis of human mesenchymal stem cells. Arthritis Rheum. 58, 1377–1388.

Nabzdyk, C., Pradhan, L., Molina, J., Perin, E., Paniagua, D., and Rosenstrauch, D. (2009). Review: auricular chondrocytes - from benchwork to clinical applications. In Vivo 23, 369–380.

Nakao, H., Jacquet, R.D., Shasti, M., Isogai, N., Murthy, A.S., and Landis, W.J. (2017). Long-term comparison between human normal conchal and microtia chondrocytes regenerated by tissue engineering on nanofiber polyglycolic acid scaffolds. Plast. Reconstr. Surg. 139, 911e–921e.

Nayyer, L., Patel, K.H., Esmaeili, A., Rippel, R.A., Birchall, M., O'Toole, G., Butler, P.E., and Seifalian, A.M. (2012). Tissue engineering: revolution and challenge in auricular cartilage reconstruction. Plast. Reconstr. Surg. 129, 1123–1137.

Nimeskern, L., van Osch, G.J.V.M., Müller, R., and Stok, K.S. (2014). Quantitative evaluation of mechanical properties in tissue-engineered auricular cartilage. Tissue Eng. Part B Rev. 20, 17–27.

Nimeskern, L., Pleumeekers, M.M., Pawson, D.J., Koevoet, W.L.M., Lehtoviita, I., Soyka, M.B., Röösli, C., Holzmann, D., van Osch, G.J.V.M., Müller, R., and Stok, K.S. (2015). Mechanical and biochemical mapping of human auricular cartilage for reliable assessment of tissue-engineered constructs. J. Biomech. 48, 1721–1729.

Otto, I.A., Melchels, F.P.W., Zhao, X., Randolph, M.A., Kon, M., Breugem, C.C., and Malda, J. (2015). Auricular reconstruction using biofabrication-based tissue engineering strategies. Biofabrication 7, 032001.

Otto, I.A., Levato, R., Webb, W.R., Khan, I.M., Breugem, C.C., and Malda, J. (2018). Progenitor cells in auricular cartilage demonstrate cartilage-forming capacity in 3D hydrogel culture. Eur. Cell. Mater. 35, 132–150.

Pampaloni, F., Reynaud, E.G., and Stelzer, E.H.K. (2007). The third dimension bridges the gap between cell culture and live tissue. Nat. Rev. Mol. Cell Biol. 8, 839–845.

Pappa, A.K., Caballero, M., Dennis, R.G., Skancke, M.D., Narayan, R.J., Dahl, J.P., and van Aalst, J.A. (2013). Biochemical properties of tissue-engineered cartilage. J. Craniofac. Surg. 25, 111–115.

Phull, A.-R., Eo, S.-H., Abbas, Q., Ahmed, M., and Kim, S.J. (2016). Applications of chondrocyte-based cartilage engineering: an overview. Biomed Res. Int. 2016, 1879837.

Pleumeekers, M.M., Nimeskern, L., Koevoet, W.L.M., Karperien, M., Stok, K.S., and van Osch, G.J.V.M. (2015). Cartilage regeneration in the head and neck area: combination of ear or nasal chondrocytes and mesenchymal stem cells improves cartilage production. Plast. Reconstr. Surg. 136, 762e.

Pomerantseva, I., Bichara, D.A., Tseng, A., Cronce, M.J., Cervantes, T.M., Kimura, A.M., Neville, C.M., Roscioli, N., Vacanti, J.P., Randolph, M.A., and Sundback, C.A. (2016). Ear-shaped stable Auricular cartilage engineered from extensively expanded chondrocytes in an immunocompetent experimental animal model. Tissue Eng. Part A 22, 197–207.

Rikkers, M., Korpershoek, J.V., Levato, R., Malda, J., and Vonk, L.A. (2021). Progenitor cells in healthy and osteoarthritic human cartilage have extensive culture expansion capacity while retaining chondrogenic properties. Cartilage 13, 129S–142S.

Roy, R., Kohles, S.S., Zaporojan, V., Peretti, G.M., Randolph, M.A., Xu, J., and Bonassar, L.J. (2004). Analysis of bending behavior of native and engineered auricular and costal cartilage. J. Biomed. Mater. Res. A 68, 597–602.

Saadeh, P.B., Brent, B., Mehrara, B.J., Steinbrech, D.S., Ting, V., Gittes, G.K., and Longaker, M.T. (1999). Human cartilage engineering: chondrocyte extraction, proliferation, and characterization for construct development. Ann. Plast. Surg. 42, 509–513.

Saim, A.B., Cao, Y., Weng, Y., Chang, C.N., Vacanti, M.A., Vacanti, C.A., and Eavey, R.D. (2000). Engineering autogenous cartilage in the shape of a helix using an injectable hydrogel scaffold. Laryngoscope 110, 1694–1697.

Schnabel, M., Marlovits, S., Eckhoff, G., Fichtel, I., Gotzen, L., Vécsei, V., and Schlegel, J. (2002). Dedifferentiation-associated changes in morphology and gene expression in primary human articular chondrocytes in cell culture. Osteoarthritis Cartilage 10, 62–70.

Schulze-Tanzil, G., Mobasheri, A., de Souza, P., John, T., and Shakibaei, M. (2004). Loss of chondrogenic potential in dedifferentiated chondrocytes correlates with deficient Shc–Erk interaction and apoptosis. Osteoarthritis Cartilage 12, 448–458.

Schuurman, W., Levett, P.A., Pot, M.W., van Weeren, P.R., Dhert, W.J.A., Hutmacher, D.W., Melchels, F.P.W., Klein, T.J., and Malda, J. (2013). Gelatin-methacrylamide hydrogels as potential biomaterials for fabrication of tissue-engineered cartilage constructs. Macromol. Biosci. 13, 551–561.

Siegel, G., Kluba, T., Hermanutz-Klein, U., Bieback, K., Northoff, H., and Schäfer, R. (2013). Phenotype, donor age and gender affect function of human bone marrow-derived mesenchymal stromal cells. BMC Med. 11, 146.

Steffen, A., Wollenberg, B., König, I.R., and Frenzel, H. (2010). A prospective evaluation of psychosocial outcomes following ear reconstruction with rib cartilage in microtia. J. Plast. Reconstr. Aesthet. Surg. 63, 1466–1473.

Sterodimas, A., de Faria, J., Correa, W.E., and Pitanguy, I. (2009). Tissue engineering and auricular reconstruction: a review. J. Plast. Reconstr. Aesthet. Surg. 62, 447–452.

Stoddart, M.J., Richards, R.G., and Alini, M. (2012). In vitro experiments with primary mammalian cells: to pool or not to pool? Eur Cell Mater 24. https://doi.org/10.22203/ecm.v024a00.

Strässler, E.T., Aalto-Setälä, K., Kiamehr, M., Landmesser, U., and Kränkel, N. (2018). Age is relative-impact of donor age on induced pluripotent stem cell-derived cell functionality. Front. Cardiovasc. Med. 5, 4.

Takebe, T., Kobayashi, S., Kan, H., Suzuki, H., Yabuki, Y., Mizuno, M., Adegawa, T., Yoshioka, T., Tanaka, J., Maegawa, J., and Taniguchi, H. (2012). Human elastic cartilage engineering from cartilage progenitor cells using rotating wall vessel bioreactor. Transplant. Proc. 44, 1158–1161.

Tay, A.G., Farhadi, J., Suetterlin, R., Pierer, G., Heberer, M., and Martin, I. (2004). Cell yield, proliferation, and postexpansion differentiation capacity of human ear, nasal, and rib chondrocytes. Tissue Eng. 10, 762–770.

Tseng, A., Pomerantseva, I., Cronce, M.J., Kimura, A.M., Neville, C.M., Randolph, M.A., Vacanti, J.P., and Sundback, C.A. (2014). Extensively expanded auricular chondrocytes form neocartilage in vivo. Cartilage 5, 241–251.

van Osch, G.J., van der Veen, S.W., and Verwoerd-Verhoef, H.L. (2001). In vitro redifferentiation of culture-expanded rabbit and human auricular chondrocytes for cartilage reconstruction. Plast. Reconstr. Surg. 107, 433–440.

van Osch, G.J.V.M., Mandl, E.W., Jahr, H., Koevoet, W., Nolst-Trenité, G., and Verhaar, J.A.N. (2004). Considerations on the use of ear chondrocytes as donor chondrocytes for cartilage tissue engineering. Biorheology 41, 411–421.

Vega, S.L., Kwon, M.Y., and Burdick, J.A. (2017). Recent advances in hydrogels for cartilage tissue engineering. Eur. Cell. Mater. 33, 59–75.

Vinod, E., Boopalan, P.R.J.V.C., and Sathishkumar, S. (2017). Reserve or resident progenitors in cartilage? Comparative analysis of chondrocytes versus chondroprogenitors and their role in cartilage repair. Cartilage 9, 171–182.

Vinod, E., Parameswaran, R., Amirtham, S.M., Rebekah, G., and Kachroo, U. (2021). Comparative analysis of human bone marrow mesenchymal stem cells, articular cartilage derived chondroprogenitors and chondrocytes to determine cell superiority for cartilage regeneration. Acta Histochem. 123, 151713.

Visscher, D.O., Gleadall, A., Buskermolen, J.K., Burla, F., Segal, J., Koenderink, G.H., Helder, M.N., and van Zuijlen, P.P.M. (2019). Design and fabrication of a hybrid alginate hydrogel/poly(ε-caprolactone) mold for auricular cartilage reconstruction. J. Biomed. Mater. Res. B Appl. Biomater. 107, 1711–1721.

Visser, J., Melchels, F.P.W., Jeon, J.E., van Bussel, E.M., Kimpton, L.S., Byrne, H.M., Dhert, W.J.A.,

Dalton, P.D., Hutmacher, D.W., and Malda, J. (2015). Reinforcement of hydrogels using three-dimensionally printed microfibres. Nat. Commun. 6, 6933.

Williams, R., Khan, I.M., Richardson, K., Nelson, L., McCarthy, H.E., Analbelsi, T., Singhrao, S.K., Dowthwaite, G.P., Jones, R.E., Baird, D.M., et al. (2010). Identification and clonal characterisation of a progenitor cell sub-population in normal human articular cartilage. PLoS One 5, e13246.

Wu, J.Z., and Herzog, W. (2002). Elastic anisotropy of articular cartilage is associated with the microstructures of collagen fibers and chondrocytes. J. Biomech. 35, 931–942.

Xue, K., Zhang, X., Qi, L., Zhou, J., and Liu, K. (2016). Isolation, identification, and comparison of cartilage stem progenitor/cells from auricular cartilage and perichondrium. Am. J. Transl. Res. 8, 732–741.

Zhang, L., He, A., Yin, Z., Yu, Z., Luo, X., Liu, W., Zhang, W., Cao, Y., Liu, Y., and Zhou, G. (2014). Regeneration of human-ear-shaped cartilage by co-culturing human microtia chondrocytes with BMSCs. Biomaterials 35, 4878–4887.

Zhang, X., Qi, L., Chen, Y., Xiong, Z., Li, J., Xu, P., Pan, Z., Zhang, H., Chen, Z., Xue, K., and Liu, K. (2019). The in vivo chondrogenesis of cartilage stem/progenitor cells from auricular cartilage and the perichondrium. Am. J. Transl. Res. 11, 2855–2865.

Zhao, S., and Fernald, R.D. (2005). Comprehensive algorithm for quantitative real-time polymerase chain reaction. J. Comput. Biol. 12, 1047–1064.

Zopf, D.A., Flanagan, C.L., Nasser, H.B., Mitsak, A.G., Huq, F.S., Rajendran, V., Green, G.E., and Hollister, S.J. (2015). Biomechanical evaluation of human and porcine auricular cartilage. Laryngoscope 125, E262–E268.

STAR★METHODS

KEY RESOURCES TABLE

REAGENT or RESOURCE	SOURCE	IDENTIFIER
Antibodies		
Collagen Type I	Abcam	ab138492; RRID:AB_2861258
Collagen Type II	DSHB	II-II6B3; RRID:AB_528165
Goat Anti-Mouse HRP	DAKO	p0447
Elastin	Abcam	Ab9519; RRID:AB_2099589
Streptavidin conjugated with HRP	DAKO	P0397
CD45-PE Mouse IgG$_1$ Clone 2D1	R&D Systems	FAB1430P; RRID:AB_2237898
CD34-PE Mouse IgG$_1$ Clone QBEnd10	R&D Systems	FAB7227P; RRID:AB_10973177
CD11b-PE Mouse IgG$_{2B}$ Clone 238446	R&D Systems	FAB16991P; RRID:AB_416844
CD79A-PE Mouse IgG$_1$ Clone 706931	R&D Systems	FAB69201P
HLA-DR-PE Mouse IgG$_1$ Clone L203	R&D Systems	FAB4869P; RRID:AB_1151931
HRP-conjugated EnVision+ for Rabbit	DAKO	K4010
CD90-APC	R&D Systems	FAB7335A
CD73-CFS	R&D Systems	5795-EN
CD105-APC	Abcam	N/A
Chemicals, Peptides, and Recombinant Proteins		
basic fibroblast growth factor (bFGF)	Peprotech	GMP100-18B
transforming growth factor β1 (TGF-β1)	Peprotech	RPN1001V
Resazurin	Alfa Aesar	62758-13-8
2-hydroxy-1-[4-(2-hydroxyethoxy)phenyl]-2-methyl-1-propanone (Irgacure 2959)	BASF	2959
Critical Commercial Assays		
RNeasy Mini Kit	Qiagen	74106
SuperScript® III Platinum SYBR Green One-Step qRT-PCR Kit	Life Technologies	11736059
Quant-iT PicoGreen dsDNA assay	Life Technologies	P7589
Oligonucleotides		
Primer sequences are listed in Table S1	This study	N/A
Software and Algorithms		
FlowJo V10	TreeStar	https://www.flowjo.com
Graphpad Prism 7	Graphpad Software	https://www.graphpad.com/scientific-software/prism/
PCRminer algorithm	Zhao and Fernald (2005)	http://118.190.66.83/miner/data_submit.htm

RESOURCE AVAILABILITY

Lead contact

Further information and requests for resources should be directed to and will be fulfilled by the lead contact, dr. Riccardo Levato (r.levato@uu.nl).

Materials availability

This study did not generate new reagents or reposited cell lines.

Data and code availability

● Data reported in this paper will be shared by the lead contact upon request.

- This paper does not report original code.

- Any additional information required to reanalyze the data reported in this paper is available from the lead contact upon request.

EXPERIMENTAL MODEL AND SUBJECT DETAILS

Human auricular cartilage

This study uses progenitor cells obtained from the auricular cartilages from human subjects. All tissues were obtained from biopsies of redundant tissue excised during surgery or from deceased donors who had donated their body to science, according to the guidelines of the Ethical Committee of the University Medical Center Utrecht. Donors have given prior informed consent to the use of their tissues for scientific research. Tissues were kindly provided by the Department of Anatomy at the University Medical Center Utrecht (The Netherlands) and the Department of Plastic, Reconstructive & Hand Surgery at the Wilhelmina Children's Hospital (Utrecht, The Netherlands). Anonymization of donated tissue was performed to ensure non-traceability of their origins. For the isolation of human auricular cartilage progenitor cells (AuCPC), fresh auricular cartilage was collected from three sources: recently deceased elderly donors (AuCPC-adult; n = 4, mean age 87.5 ± 12.3, range 69–94 years; specifically: male, 94 y/o, male, 93 y/o, female, 69 y/o, female, 94 y/o), healthy normal cartilage of pediatric patients removed during protruding ear correction surgery (AuCPC-pediatric; n = 3, mean age 7.7 ± 2.1, range 6–10 years; specifically; male, 6 y/o, female, 10 y/o, female, 7 y/o), and the cartilage remnants of pediatric patients with microtia, removed during ear reconstruction surgery (AuCPC-microtia; n = 3, mean age 10 ± 3.6, range 7–14 years; specifically: male, 7 y/o, male, 9 y/o, male, 14 y/o).

Isolation of cartilage progenitor cells

Harvested auricles from deceased donors were thoroughly washed with water and soap and subsequently disinfected by soaking in Betadine® (Meda Pharma, Amstelveen, The Netherlands). Under sterile conditions, the auricular skin and subcutaneous tissue were removed using a scalpel. Microtia and protruding ear cartilage remnants were washed in phosphate-buffered saline (PBS) and subsequently stripped of any remaining subcutaneous tissue. In all cases, the perichondrial layer was removed using a scraping technique as previously described (Otto et al., 2018). Cartilage chips were sectioned off the exposed cartilage layer, washed in PBS substituted with 0.3% gentamycin (Lonza, USA) and minced into 1 mm^2 pieces. The minced cartilage tissue was enzymatically digested in 0.2% pronase (Roche, USA) solution for 2 hours followed by 0.075% collagenase type II (Worthington Chemical Corporation, Lakewood, NJ, USA) digestion for 16 hours at 37°C. The solution was then filtered through a 100 μm cell strainer and centrifuged for 5 minutes at 300 ×g to obtain a cell pellet. The pelleted cells were resuspended in Dulbecco's modified Eagle medium (DMEM; 31966, Gibco, The Netherlands) and subjected to a fibronectin adhesion assay as previously described (Williams et al., 2010; Dowthwaite et al., 2004). Briefly, cells were plated at a density of 500 cells/cm^2 in fibronectin-coated culture flasks and incubated for 20 minutes at 37°C. The non-adherent cells were carefully removed and the remaining attached cells were cultured in chondroprogenitor expansion media, consisting of DMEM supplemented with 10% v/v fetal bovine serum (FBS; Lonza), 0.2 mM L-ascorbic acid 2-phosphate (Sigma-Aldrich, The Netherlands), 100 U/mL penicillin (Life Technologies, The Netherlands), 100 μg/mL streptomycin (Life Technologies) and 5 ng/mL basic fibroblast growth factor (bFGF; Peprotech, London, UK). Cells were collected and stored at each passage up till passage 4 in liquid nitrogen until further use.

METHOD DETAILS

Visualization of cell morphology

Morphological evaluation of AuCPC during expansion was carried out from passage 0 through 5 by light microscopy imaging (Leica DMi1, Germany). Colony formation was captured during passage 0. At subsequent passages, images were taken at day 4 of culture.

Evaluation of growth rates

Proliferation rates during expansion were determined at passages 1–5 using a resazurin assay to estimate cell number indirectly through measuring cellular mitochondrial metabolic activity (Czekanska, 2011). AuCPC cells from all donors were cultured up to confluency at every passage and subsequently plated at a density of 5.0 × 10^3 in 12-well tissue plates (n = 4 per donor), where they were cultured in progenitor

expansion medium supplemented with 5 ng/mL bFGF. On days 1, 3, 4–10 (or beyond if cell numbers had not reached plateau growth phase) the assay was performed by incubating the cells in 10X diluted resazurin solution (Alfa Aesar, Germany) for 3 hours at 37°C. Fluorescence of resorufin, the metabolically reduced compound, was measured at 544 nm excitation and 570 nm emission using a spectrofluorometer (Fluoroskan Ascent FL; ThermoFisher, USA). A calibration curve was determined by plating known cell densities and measuring the absorbance at day 1. Population doublings were calculated using the following equation, where $x0$ is the starting cell number and N is the cell number at time of measurement:

$$Population\ doublings\ =\ \frac{\log\left(\frac{N}{x0}\right)}{\log 2}$$

Stem cell marker expression

Flow cytometry was used to determine stem cell marker expression of the isolated cell population of each donor, using a marker panel consisting of CD45, CD34, CD73, CD90 and CD105 (Dominici et al., 2006). For each donor, 1.0×10^5 AuCPCs at passage 4 were washed in 1X Flow Cytometry Staining Buffer (R&D Systems, USA) and incubated for 45 minutes at room temperature in the dark with either CD90-APC (R&D Systems), CD105-APC (Abcam, UK), CD73-CFS (R&D Systems) or a cocktail of negative markers conjugated to PE (consisting of CD45-PE Mouse IgG_1 Clone 2D1, CD34-PE Mouse IgG_1 Clone QBEnd10, CD11b-PE Mouse IgG_{2B} Clone 238446, CD79A-PE Mouse IgG_1 Clone 706931, HLA-DR-PE Mouse IgG_1 Clone L203; R&D Systems). Labeled cells were washed once with and subsequently resuspended in 100 μL Staining Buffer, and analyzed using a BD FACSCanto II (BD Biosciences, USA). Dead cells were excluded with 4′,6-diamidino-2-phenylindole (DAPI; Sigma). Corresponding isotype antibodies were used as controls to exclude non-specific binding. Results were analyzed using FlowJo V10 data analysis software package (TreeStar, USA).

Assessment of multipotency

Retention of multipotency of hAuCPCs during expansion was evaluated through an *in vitro* trilineage differentiation assay at passages 3, 4 and 5. Cells were directed towards the osteogenic, adipogenic or chondrogenic lineage through the appropriate differentiation media. For adipogenic and osteogenic differentiation, cells were plated in duplicate at a density of 3×10^5 cells per well in 6-well tissue culture plates and cultured until sub-confluency in chondroprogenitor expansion medium. When cell-cell contact was observed, cells were cultured in differentiation media for 21 and 28 days, respectively. Osteogenic differentiation medium consisted of αMEM (Gibco) supplemented with 10% v/v FBS (Lonza), 100 U/mL penicillin (Life Technologies), 100 μg/mL streptomycin (Life Technologies), 0.2 mM L-ascorbic acid 2-phosphate (Sigma-Aldrich), 20 mM β-glycerol phosphate (Sigma-Aldrich) and 100 nM dexamethasone (Sigma-Aldrich). Adipogenic medium consisted of αMEM (Gibco) supplemented with 10% v/v FBS (Lonza), 100 U/mL penicillin (Life Technologies), 100 μg/mL streptomycin (Life Technologies), 0.01 mM indomethacin (Sigma-Aldrich), 83 mM 3-Isobutyl-1-metylxanthine (Sigma-Aldrich) and 1.72 μm bovine pancreas-derived insulin (Sigma-Aldrich). For chondrogenic differentiation, cells were pelleted at a density of 2.5×10^5 in 15 mL Falcon® tubes by centrifugation at 300 ×g for 5 minutes. The pellets were subsequently cultured for 21 days in chondrogenic differentiation medium, consisting of DMEM supplemented with 1% v/v ITS+ Premix (insulin-transferrin-selenous acid; Corning, USA), 0.2 mM L-ascorbic acid 2-phosphate (Sigma-Aldrich), 100 U/mL penicillin (Life Technologies), 100 μg/mL streptomycin (Life Technologies), 100 nM dexamethasone (Sigma-Aldrich) and 10 ng/mL transforming growth factor β1 (TGF-β1; Peprotech). Culture medium was refreshed every 3 days.

At the end of the culture period, cells and pellets were washed with PBS and fixed in 4% neutral-buffered formalin (NBF; Klinipath, UK). Pellets were subsequently embedded in paraffin and sectioned into 5 μm-thick slices. Osteogenic differentiation was determined by observing calcified matrix deposition using alizarin red S staining (Sigma-Aldrich). Adipogenic commitment was visualized by oil red O staining (Sigma-Aldrich) demonstrating the formation of intracellular lipid vesicles. Chondrogenic differentiation was assessed by staining sectioned pellets with safranin O (Sigma-Aldrich) to visualize glycosaminoglycan deposition.

Fabrication of 3D cell-laden hydrogel constructs

Gelatin methacryloyl (gelMA) was synthesized according to a previously published protocol, as used as a platform to produce hydrogels for 3D tissue culture (Melchels et al., 2014). Briefly, gelatin type A (obtained

from porcine skin; Sigma-Aldrich) in PBS was functionalized with methacrylic anhydride groups to achieve an 80% degree of functionalization of the available primary amines. Subsequently, a 10% w/v solution of gelMA was supplemented with 0.1% w/v 2-hydroxy-1-[4-(2-hydroxyethoxy)phenyl]-2-methyl-1-propanone (Irgacure 2959; BASF, Ludwigshafen, Germany) as a photoinitiator. AuCPCs of each donor were expanded to passage 4 and were encapsulated in the hydrogel at a density of 1.5×10^7 cells/mL at 37°C. The cell-laden gel was cast into a custom-made Teflon™ mold and subsequently subjected to UV-radiation for 15 minutes (wavelength λ = 365 nm, intensity E = 7 mW/cm², at height of 12 cm; CL-1000L UV Crosslinker, UVP, UK) to allow free-radical polymerization crosslinking of the hydrogel, producing cylindrical samples (diameter = 6 mm, height = 2 mm). As controls, cell-free hydrogel samples were prepared under the same conditions. All samples were cultured in chondrogenic differentiation medium for 1, 28 and 56 days at 37°C and 5% CO^2 and receiving fresh media 3 times per week.

Gene expression of cartilage markers

After 1 and 56 days of culture, the relative gene expression of cartilage markers in cell-laden hydrogels (n = 3) was evaluated through qPCR. Analyzed markers included aggrecan (ACAN), cartilage oligomeric matrix protein (COMP), collagen type I (COL1A1), collagen type II (COL2A1), collagen type X (COLXA1), and runt-related transcription factor 2 (RUNX2). Expression levels of these markers were normalized against the housekeeping gene hypoxanthine phosphoribosyltransferase (HPRT1). Primer sequences for each transcript are reported in Table S1. At each given time point, cell-laden hydrogel samples were mechanically ground in RLT buffer (Qiagen, Germany) and mRNA was isolated from the lysate using the RNeasy Mini Kit (Qiagen) and subsequently quantified with a Nanodrop 2000 (Thermo Scientific, The Netherlands). A SuperScript® III Platinum SYBR Green One-Step qRT-PCR Kit (Life Technologies) was used for mRNA amplification and cDNA synthesis, which was performed with a LightCycler® 96 (Roche). Relative gene expression, Ct and efficiency values were calculated using the PCRminer algorithm (Zhao and Fernald, 2005).

Biochemical analysis of cell-laden hydrogels

After 1, 28 and 56 days of culture, 4–6 replicates of each group of cell-laden hydrogels were collected for quantification of DNA and GAG content. Samples were frozen at −20°C and subsequently lyophilized. The wet and dry weights were recorded during this process to calculate the final mass of the lyophilized samples. Subsequently, samples were digested overnight at 60°C in 200 μL papain digestion buffer (P3125; Sigma-Aldrich), consisting of 0.2 M NaH_2PO_4 (Merck, USA) and 0.01 M ethylenediaminetetraacetic acid (EDTA; VWR, USA) in milliQ water (pH = 6.0), supplemented with 250 μL/mL papain solution (48 units/ mg of protein; Sigma-Aldrich) and 0.01 M cysteine (C9768; Sigma-Aldrich).

Total double-stranded DNA (dsDNA) content was quantified using a Quant-iT PicoGreen dsDNA assay (Life Technologies). Fluorescence was measured at 485 nm excitation and 520 nm emission with a spectrofluorometer (Fluoroskan Ascent FL; ThermoFisher). Results were corrected for the dilution factor and compared to a standard of known concentrations of DNA.

Glycosaminoglycan content, as a measure of cartilage-specific matrix production, was quantified using a dimethylmethylene blue (DMMB; Sigma-Aldrich; pH = 3.0) assay. The 525/595 nm absorbance ratio of the reagent was measured with a VersaMax plate reader (Molecular Devices, Winnersh, UK). The content of sulphated GAG (sGAG) was derived using a standard of known concentrations of chondroitin sulphate C and corrected for the dilution factor.

sGAG and dsDNA content in each sample were both normalized against the dry weight of the sample. The ratio of sGAG per dsDNA was calculated to display the cartilage-specific matrix-production activity of single cells in the hydrogel.

Compressive mechanical testing

After 1, 28 and 56 days of culture, 4–6 replicates per time point were collected for each donor and subjected to an unconfined uniaxial compression test to evaluate the mechanical properties. Using a dynamic mechanical analyzer (DMA Q800; TA Instruments, Asse, Belgium), samples were compressed at a −20%/ min strain rate to a maximum of −30% strain. The Young's modulus of each sample was calculated as the slope of the initials linear segment (10–15% strain) of the stress-strain curve.

Histology and immunohistochemistry

Deposition of key components of cartilage extracellular matrix in cell-laden hydrogels after 1, 28 and 56 days of culture was visualized by histology and immunohistochemistry on formalin-fixed, paraffin-embedded samples. After fixation in 4% neutral-buffered formalin, samples were dehydrated through a graded ethanol series (70%, 96% and 100% ethanol), cleared in xylene and embedded in paraffin. Samples were sectioned into 5 µm-thick slices and deparaffinized prior to staining. A triple stain consisting of Weigert's hematoxylin (cell nuclei), fast green (collagens) and safranin O (proteoglycans) was performed to visualize cartilage glycosaminoglycan deposition. Deposition of collagens was evaluated by immunohistochemistry, with appropriate antibodies for collagen type I (ab138492, 1:400; Abcam) and collagen type II (II-II6B3; DSHB, Iowa, USA). Appropriate IgG were used as isotype controls. After deparaffinization, samples were first treated with 0.3% v/v H_2O_2 to block endogenous peroxidases. Antigen retrieval was performed with 1 mg/mL pronase (Roche) and 10 mg/mL hyaluronidase (H2126; Sigma-Aldrich), both applied for 30 minutes at 37°C. Subsequently, the tissue sections were blocked with bovine serum albumin (BSA, 5% w/v in PBS) for 1 hour at room temperature. Then, the primary antibodies were incubated overnight at 4°C, after which an HRP-tagged secondary antibody was applied for 1 hour at room temperature. For the collagen type II staining, Goat Anti-Mouse HRP (p0447, 1:200; DAKO) was used, and for the collagen type I staining HRP-conjugated EnVision+ for Rabbit (K4010; DAKO) was used. The staining was developed with 3,3-diaminobenzidine-horseradish peroxidase (Sigma-Aldrich) and cell nuclei were counterstained with Mayer's hematoxylin. The formation of elastin was also evaluated by immunohistochemistry. After deparaffinization and blocking, antigen retrieval was performed with 0.25% trypsin in EDTA (25200; Gibco) applied for 30 minutes at 37°C. Then, tissue sections were blocked with BSA for 30 minutes at room temperature. The primary antibody (Ab9519, 1:20; Abcam), Biotinylated Anti-Mouse IgG (RPN1001V, 1:200; GE Healthcare), and streptavidin conjugated with HRP (P0397, 1:500; DAKO) were subsequently applied, each for 1 hour at room temperature, with washing in between. The staining was developed with 3,3-diaminobenzidine-horseradish peroxidase and cell nuclei were counterstained with Mayer's hematoxylin. All sections were mounted in DPX mounting media (Millipore, USA) and imaged using a light microscope (Olympus BX51; Olympus, Germany).

QUANTIFICATION AND STATISTICAL ANALYSIS

Quantitative results are expressed as mean ± standard error of the mean (SEM). Quantitative analyses were performed through two-way ANOVA with a Bonferroni post-hoc test. Statistical analyses were carried out using Graphpad Prism 7 (Graphpad Software, USA). A value of $p < 0.05$ was considered statistically significant.